

1

2 *Supplement of*

3 **Intense biomass burning emissions and rapid nitrate formation**
4 **drive severe haze formation in Sichuan basin, China: insights**
5 **from aerosol mass spectrometry**

6 Zhier Bao et al.

7 *Correspondence to:* Yang Chen (chenyang@cigit.ac.cn)

8

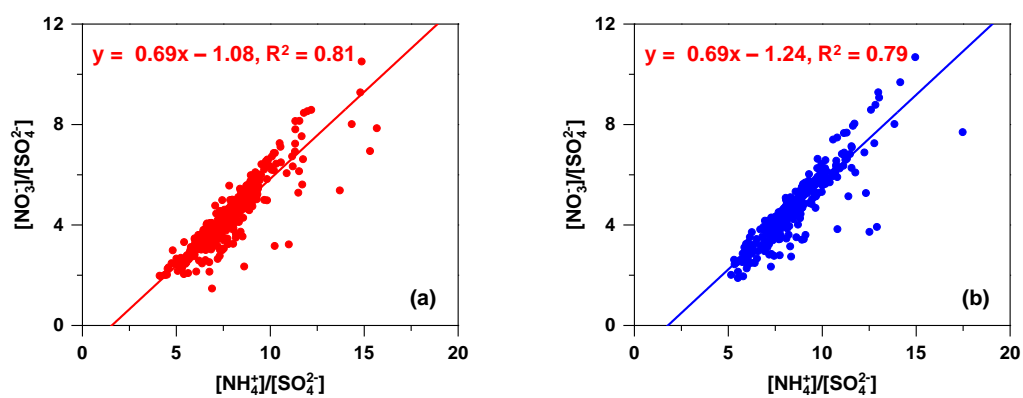
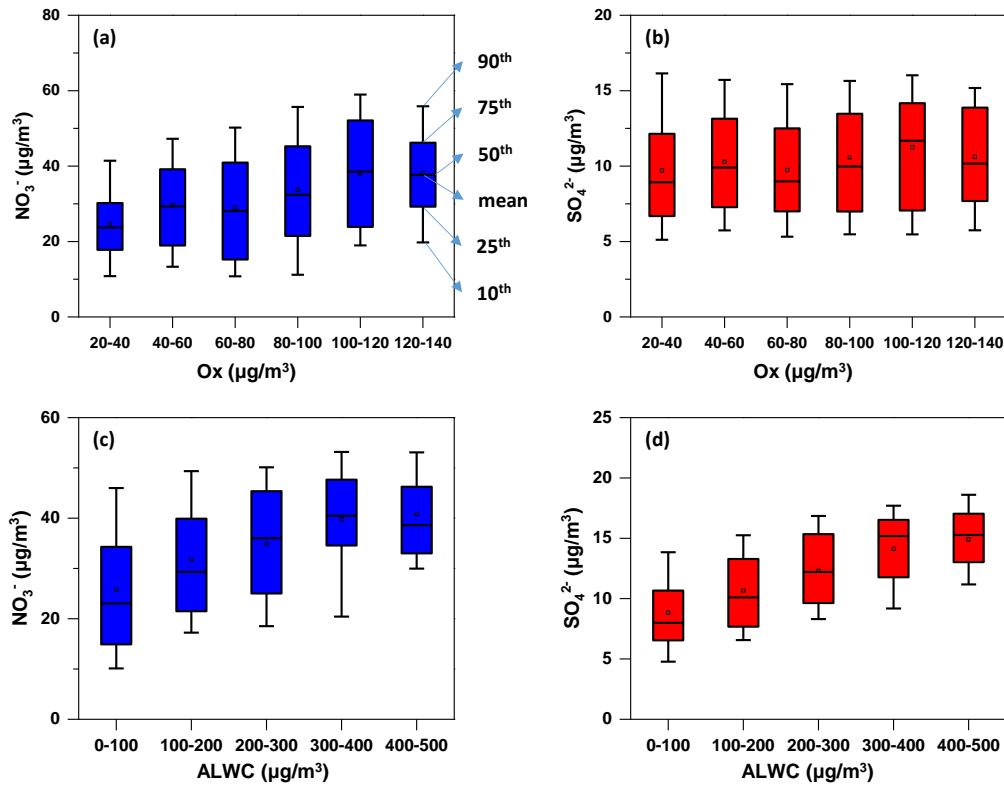


Fig. S1 Molar ratios of nitrate to sulphate vs. ammonium to sulphate during (a) daytime and (b) nighttime



15

16

Fig. S2 Variation of (a), (c) nitrate and NOR and (b), (d) sulphate and SOR as Ox/ALWC

17

increases. The data of nitrate and sulphate concentrations were grouped into different bins

18

according to 20 µg/m³ increment of Ox in (a) and (b), and 100 µg/m³ increment of ALWC in (c)

19

and (d). The mean (square), 50th (horizontal line inside the box), 25th and 75th percentiles (lower

20

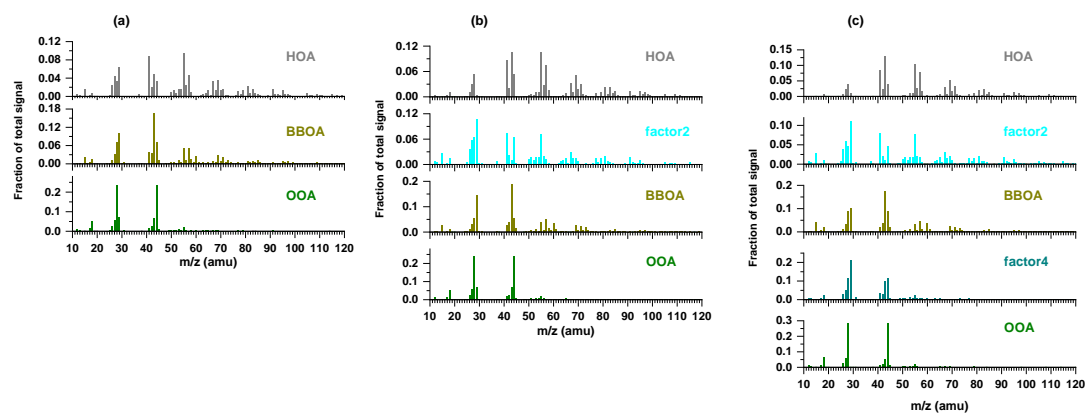
and upper box), and 10th and 90th percentiles (lower and upper whiskers) of the box chart are

21

marked in (a).

22

23



24

25 Fig. S3 Mass spectrum profile of OA factors resolved by PMF for (a) 3-, (b) 4-, and (c) 5-factor
 26 solutions

27

28

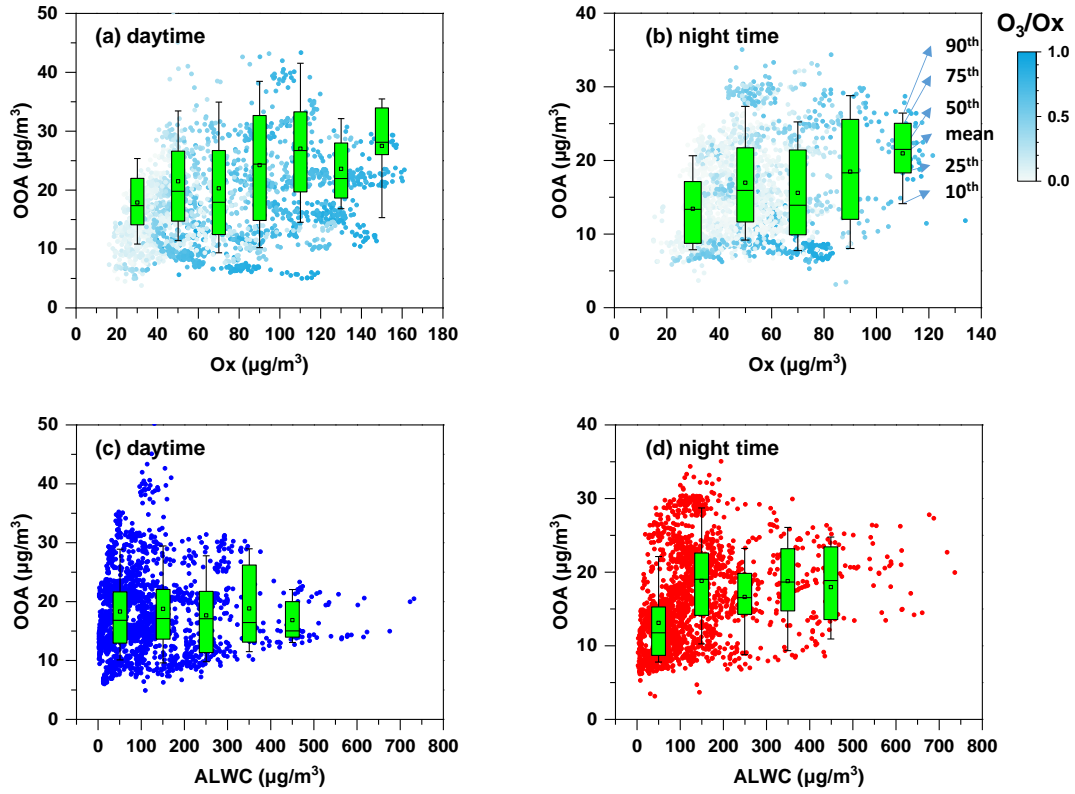
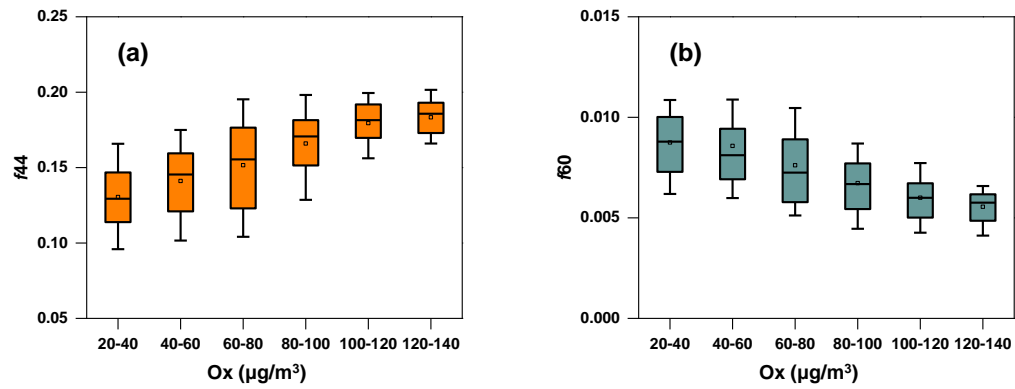


Fig. S4 OOA concentration as a function of (a) Ox and (c) ALWC during daytime. (b) and (d) are the same as (a) and (c) but during nighttime. The data of OOA concentration are grouped into different bins according to $20 \mu\text{g}/\text{m}^3$ increment of Ox and $100 \mu\text{g}/\text{m}^3$ increment of ALWC during both daytime and nighttime. The colour scale represents O_3/Ox ratios in (a) and (b). The mean (square), 50th (horizontal line inside the box), 25th and 75th percentiles (lower and upper box), and 10th and 90th percentiles (lower and upper whiskers) of the box chart are marked in (b).

40



41

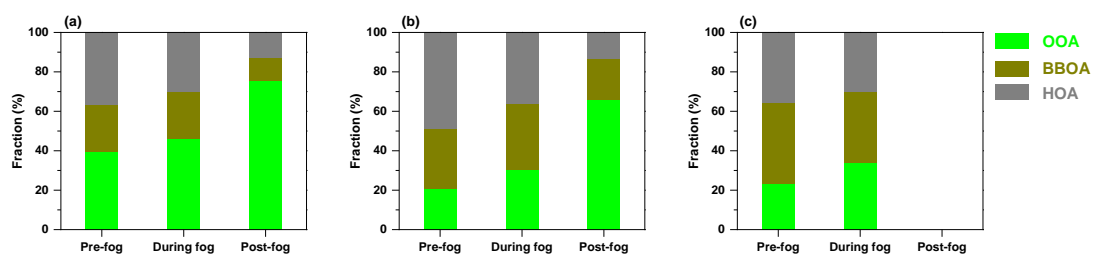
42 Fig. S5 Box chart of (a) f_{44} and (b) f_{60} as a function of Ox concentration. The data are grouped

43 into different bins according to $20 \mu\text{g}/\text{m}^3$ increment of Ox

44

45

46



47

48 Fig. S6 Relative contribution of OOA, BBOA, and HOA to OA during the evolution of (a) F1, (b)

49

F2, and (c) F3.

50

51

Table S1 Summary of mass concentrations of PM_{2.5} compositions measured during winter in different cities.

Species	This study ^a	Chengdu ^b	Chongqing ^b	Xi'an ^c	Changzhou	Beijing ^d
OA	39.2 ± 3.9	N.A.	N.A.	64.2 ± 40.6	31.2 ± 11.9	103 ± 33
NO ₃ ⁻	29 ± 14	33.4 ± 29.5	15.8 ± 9.5	27.7 ± 20.4	24.1 ± 11.8	43 ± 11
NH ₄ ⁺	15.1 ± 6.4	12 ± 7.9	11.3 ± 5.2	12.5 ± 9.1	13.1 ± 3.7	14.9 ± 5.1
SO ₄ ²⁻	10 ± 4.2	16.6 ± 13	17.5 ± 7.4	17.6 ± 14.2	18.7 ± 7.6	47 ± 15
Cl ⁻	5.2 ± 4.1	N.A.	1.6 ± 1.2	5.1 ± 4.0	N.A.	35.4 ± 7.9
Reference		(Huang et al., 2021)	(Wang et al., 2018)	(Duan et al., 2021)	(Ye et al., 2017)	(Elser et al., 2016)

^a The data of rainy hours (0:00-9:00 25 December, 2021 & 0:00-8:00 1 January, 2022) were removed.

^b The concentrations of water-soluble inorganic ions were measured by an ion chromatography, while the compositions in other cities listed in the table were measured by AMS.

^c The concentrations of different compositions were measured before COVID-19 lockdown.

^d The concentrations of different compositions were measured during extreme haze episodes.

62

63

Table S2 Description of the PMF solutions

Factor numbers	f _{peak}	Q/Q _{exp}	Comment
2	0	3.13	Too few factors and large residuals.
3	0	2.64	<p>Optimum PMF solution. Q/Q_{exp} decreases by 15.7 %. Temporal profile and diurnal variation of different factors are consistent with external tracers. The factors (HOA, BBOA, and OOA) resolved also represent major OA sources around the observation site.</p> <p>Q/Q_{exp} decreases by 14.8 %. A new factor (factor2 in Fig. S4 (b)) with high m/z 55/ m/z 57, which makes itself look like cooking organic aerosol (COA), is separated.</p> <p>However, the diurnal profile of this factor does not show apparent peaks at noon and in the evening. The observation site is not affected by intense cooking emissions either.</p> <p>Q/Q_{exp} decreases by 10 %. OOA is split into two factors with similar time series. One of the factors (factor4 in Fig. S4 (c)) has too low m/z 44 signal intensity, which is not reasonable for OOA.</p>
4	0	2.25	
5	0	2.03	

64

65

66

67

68 Table S3 Summary of meteorological parameters, mass concentrations of PM_{2.5} species, OA

69 factors and elemental ratios during different episodes.

	H1	H2	H3	F1	F2	F3	Overall
Meteorological Parameters							
T (°C)	8.2 ± 2.7	6.6 ± 2.8	8.0 ± 2.4	6.2 ± 2.3	1.5 ± 3.2	4.7 ± 1.3	7.3 ± 2.8
RH (%)	80.7 ± 11.3	81.5 ± 11.7	79.7 ± 12.4	99.9 ± 0.3	99.0 ± 1.4	99.5 ± 0.7	81.0 ± 12.4
WS (m/s)	0.7 ± 0.5	0.7 ± 0.4	0.7 ± 0.4	0.9 ± 0.4	0.7 ± 0.2	0.6 ± 0.2	0.7 ± 0.5
SR (W/m ²) ^a	297 ± 156	318 ± 157	276 ± 162	470	500	75	276 ± 164
PM _{2.5} species (µg/m ³)							
Org	45.6 ± 18.4	42.1 ± 11.5	42.2 ± 11.8	53.3 ± 12.8	45.0 ± 12.7	45.4 ± 8.4	39.2 ± 15.7
NO ₃ ⁻	34.3 ± 17.4	33.5 ± 11.1	30.2 ± 11.0	41.1 ± 17.8	22.3 ± 12.7	23.0 ± 4.9	29.0 ± 13.9
SO ₄ ²⁻	10.5 ± 4.7	11.5 ± 3.4	10.3 ± 3.8	14.6 ± 6.7	10.3 ± 2.2	13.0 ± 6.1	10.1 ± 4.2
NH ₄ ⁺	16.9 ± 7.6	17.1 ± 5.0	15.8 ± 5.5	21.3 ± 8.6	15.3 ± 3.8	13.6 ± 2.5	15.1 ± 6.4
Chl	5.8 ± 3.3	5.1 ± 2.8	5.9 ± 4.4	8.3 ± 3.6	16.2 ± 10.9	8.1 ± 2.7	5.2 ± 4.1
BC	6.7 ± 2.6	6.2 ± 2.3	7.1 ± 2.2	8.3 ± 1.9	9.3 ± 2.8	9.3 ± 1.0	6.2 ± 2.8
OA (µg/m ³)							
HOA	11.7 ± 7.6	10.5 ± 6.9	8.6 ± 5.1	13.9 ± 4.6	16.3 ± 7.7	11.0 ± 2.9	8.9 ± 6.5
BBOA	7.7 ± 5.5	10.0 ± 4.7	10.6 ± 4.6	11.2 ± 3.8	14.7 ± 5.2	13.0 ± 3.0	8.9 ± 5.4
OOA	18.3 ± 7.4	20.5 ± 6.9	15.5 ± 4.4	22.3 ± 10.1	12.8 ± 5.1	12.1 ± 2.7	16.3 ± 6.8
Elemental ratios ^b							
O/C	0.70 ± 0.14	0.71 ± 0.14	0.68 ± 0.12	0.66 ± 0.13	0.54 ± 0.13	0.55 ± 0.06	0.71 ± 0.14
H/C	1.54 ± 0.03	1.56 ± 0.02	1.58 ± 0.02	1.56 ± 0.01	1.59 ± 0.01	1.59 ± 0.01	1.56 ± 0.09
$\overline{\text{OS}}_c$	-0.12 ± 0.39	-0.14 ± 0.28	-0.23 ± 0.25	-0.23 ± 0.26	-0.51 ± 0.22	-0.48 ± 0.12	-0.14 ± 0.31

70 ^a The daily maximum was used for calculating the average values during different episodes71 ^b The O/C and H/C were determined by the parameterization proposed by Canagaratna et al. (2015).72 The $\overline{\text{OS}}_c$ was calculated as 2O/C - H/C recommended by (Heald et al., 2010).

73

74

75

76 **References**

77

78 Canagaratna, M. R., Jimenez, J. L., Kroll, J. H., Chen, Q., Kessler, S. H., Massoli, P., Hildebrandt Ruiz,
79 L., Fortner, E., Williams, L. R., Wilson, K. R., Surratt, J. D., Donahue, N. M., Jayne, J. T., and
80 Worsnop, D. R.: Elemental ratio measurements of organic compounds using aerosol mass
81 spectrometry: characterization, improved calibration, and implications, *Atmos. Chem. Phys.*, 15,
82 253-272, [https://doi.org/ 10.5194/acp-15-253-2015](https://doi.org/10.5194/acp-15-253-2015), 2015.

83 Duan, J., Huang, R., Chang, Y., Zhong, H., Gu, Y., Lin, C., Hoffmann, T., and O'Dowd, C.: Measurement
84 report of the change of PM_{2.5} composition during the COVID-19 lockdown in urban Xi'an: Enhanced
85 secondary formation and oxidation, *Sci. Total Environ.*, 791, 148126, [https://doi.org/](https://doi.org/10.1016/j.scitotenv.2021.148126)
86 10.1016/j.scitotenv.2021.148126, 2021.

87 Elser, M., Huang, R., Wolf, R., Slowik, J. G., Wang, Q., Canonaco, F., Li, G., Bozzetti, C., Daellenbach,
88 K. R., Huang, Y., Zhang, R., Li, Z., Cao, J., Baltensperger, U., El-Haddad, I., and Prévôt, A. S. H.:
89 New insights into PM_{2.5} chemical composition and sources in two major cities in China during
90 extreme haze events using aerosol mass spectrometry, *Atmos. Chem. Phys.*, 16, 3207-3225,
91 [https://doi.org/ 10.5194/acp-16-3207-2016](https://doi.org/10.5194/acp-16-3207-2016), 2016.

92 Heald, C. L., Kroll, J. H., Jimenez, J. L., Docherty, K. S., DeCarlo, P. F., Aiken, A. C., Chen, Q., Martin,
93 S. T., Farmer, D. K., and Artaxo, P.: A simplified description of the evolution of organic aerosol
94 composition in the atmosphere, *Geophys. Res. Lett.*, 37, [https://doi.org/ 10.1029/2010GL042737](https://doi.org/10.1029/2010GL042737),
95 2010.

96 Huang, X., Zhang, J., Zhang, W., Tang, G., and Wang, Y.: Atmospheric ammonia and its effect on PM_{2.5}
97 pollution in urban Chengdu, Sichuan Basin, China, *Environ. Pollut.*, 291, 118195, [https://doi.org/](https://doi.org/10.1016/j.envpol.2021.118195)
98 10.1016/j.envpol.2021.118195, 2021.

99 Wang, H., Tian, M., Chen, Y., Shi, G., Liu, Y., Yang, F., Zhang, L., Deng, L., Yu, J., Peng, C., and Cao,
100 X.: Seasonal characteristics, formation mechanisms and source origins of PM_{2.5} in two megacities in
101 Sichuan Basin, China, *Atmos. Chem. Phys.*, 18, 865-881, [https://doi.org/ 10.5194/acp-18-865-2018](https://doi.org/10.5194/acp-18-865-2018),
102 2018.

103 Ye, Z., Liu, J., Gu, A., Feng, F., Liu, Y., Bi, C., Xu, J., Li, L., Chen, H., Chen, Y., Dai, L., Zhou, Q., and
104 Ge, X.: Chemical characterization of fine particulate matter in Changzhou, China, and source
105 apportionment with offline aerosol mass spectrometry, *Atmos. Chem. Phys.*, 17, 2573-2592,
106 [https://doi.org/ 10.5194/acp-17-2573-2017](https://doi.org/10.5194/acp-17-2573-2017), 2017.

107